

# ZH production in gluon fusion at NLO QCD

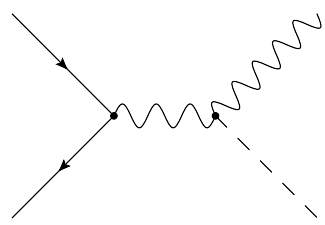
Matthias Kerner  
HP2, Newcastle, 21 Sep 2022

in collaboration with  
L. Chen, J. Davies, G. Heinrich, S. Jones, G. Mishima, J. Schlenk, M. Steinhauser

*JHEP 08 (2022) 056 (arXiv:2204.05225 )*

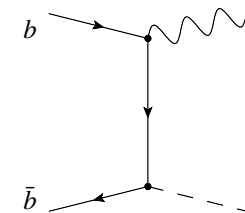
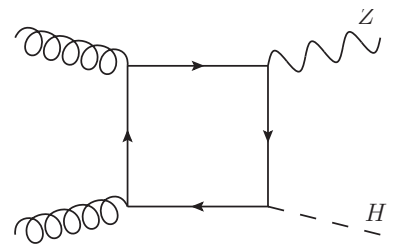
# Introduction – ZH Production Modes

ZH production modes



NNLO: Brein, Djouadi, Harlander 03

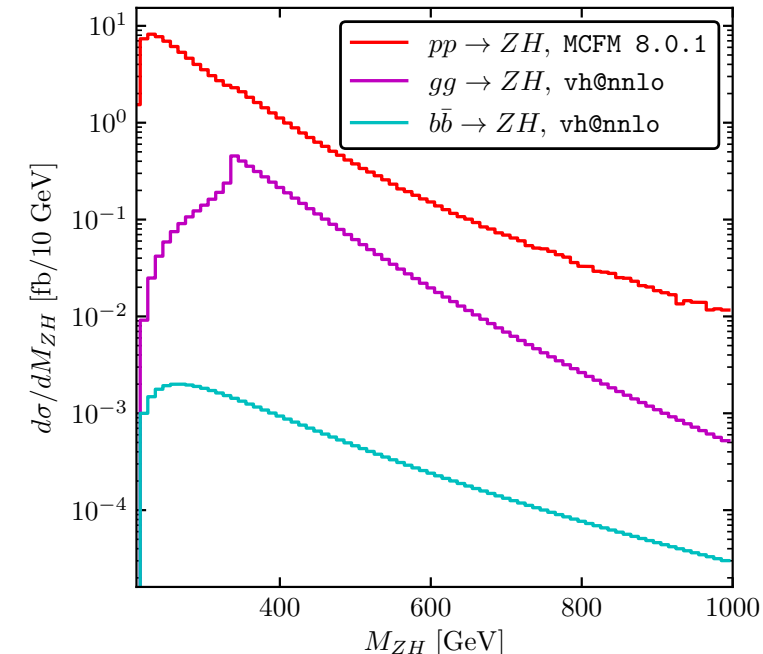
N<sup>3</sup>LO: Baglio, Mistlberger, Szafron 22



NNLO

Ahmed, Ajjath, Chen, Dhani,  
Mukherjee, Ravindran 19

[Harlander, Klappert, Liebler, Simon 18]



Gluon-induced production:

- Contribution to total cross section ~10%
- Large scale uncertainties

quark-initiated production  
known with high accuracy:

NNLO: Brein, Harlander, Wiesemann, Zirke; Ferrera, Grazzini, Somogyi,

Tramontano; Campbell, Ellis, Williams; Gauld, Gehrmann-De Ridder,  
Glover, Huss, Majer

NLO EW(+QCD): Ciccolini, Denner, Dittmaier, Kallweit, Krämer,  
Mück; Granata, Lindert, Oleari, Pozzorini; Obul, Dulat, Hou, Tursun,  
Yulkun

N<sup>3</sup>LO: Baglio, Mistlberger, Szafron 22

Uncertainties in ZH, WH measurements

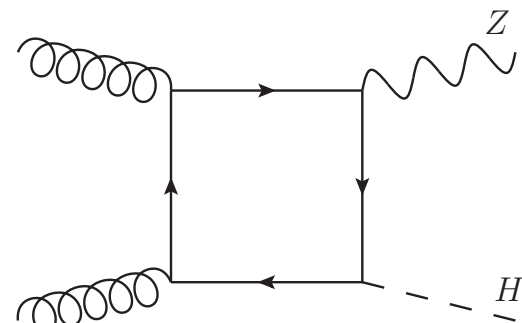
ATLAS 2007.02873

	Signal
Cross-section (scale)	0.7% ( $qq$ ), 25% ( $gg$ )
$H \rightarrow b\bar{b}$ branching fraction	1.7%
Scale variations in STXS bins	3.0%–3.9% ( $qq \rightarrow WH$ ), 6.7%–12% ( $qq \rightarrow ZH$ ), 37%–100% ( $gg \rightarrow ZH$ )
PS/UE variations in STXS bins	1%–5% for $qq \rightarrow VH$ , 5%–20% for $gg \rightarrow ZH$
PDF+ $\alpha_S$ variations in STXS bins	1.8%–2.2% ( $qq \rightarrow WH$ ), 1.4%–1.7% ( $qq \rightarrow ZH$ ), 2.9%–3.3% ( $gg \rightarrow ZH$ )
$m_{bb}$ from scale variations	M+S ( $qq \rightarrow VH, gg \rightarrow ZH$ )
$m_{bb}$ from PS/UE variations	M+S
$m_{bb}$ from PDF+ $\alpha_S$ variations	M+S
$p_T^V$ from NLO EW correction	M+S

# Introduction – $gg \rightarrow ZH$ : Calculations at LO and NLO

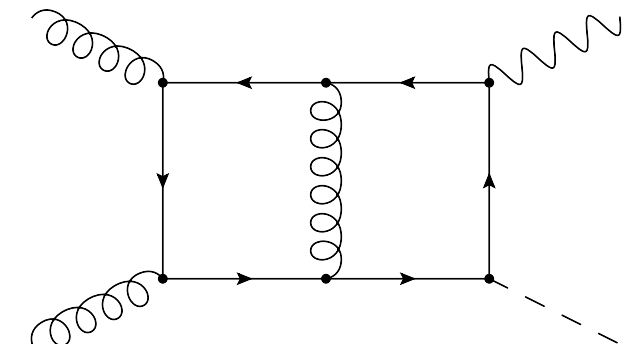
Leading Order

[Dicus, Kao 88; Kniehl 90]



NLO in  $m_t \rightarrow \infty$  limit

[Altenkamp, Dittmaier, Harlander, H. Rzehak, Zirke 12]



Virtual corrections with  $m_t$  dependence

- Expansion in large  $m_t$ , up to  $1/m_t^8$ , improved by Padé approx.  
[Hasselhuhn, Luthe, Steinhauser 17]

- expansion in small and large  $m_t$ , up to  $1/m_t^{10}, m_t^{32}$  + Padé approx.  
[Davies, Mishima, Steinhauser 20]
- numerical evaluation using pySecDec  
[Chen, Heinrich, Jones, MK, Klappert, Schlenk 20]

- expansion in small  $p_T$  up to  $p_T^4$   
[Alasfar, Degrassi, Giardino, Gröber, Vitti 21]
- combine expansions in small  $p_T$  and small  $m_t$   
[Bellafronte, Degrassi, Giardino, Gröber, Vitti 22]

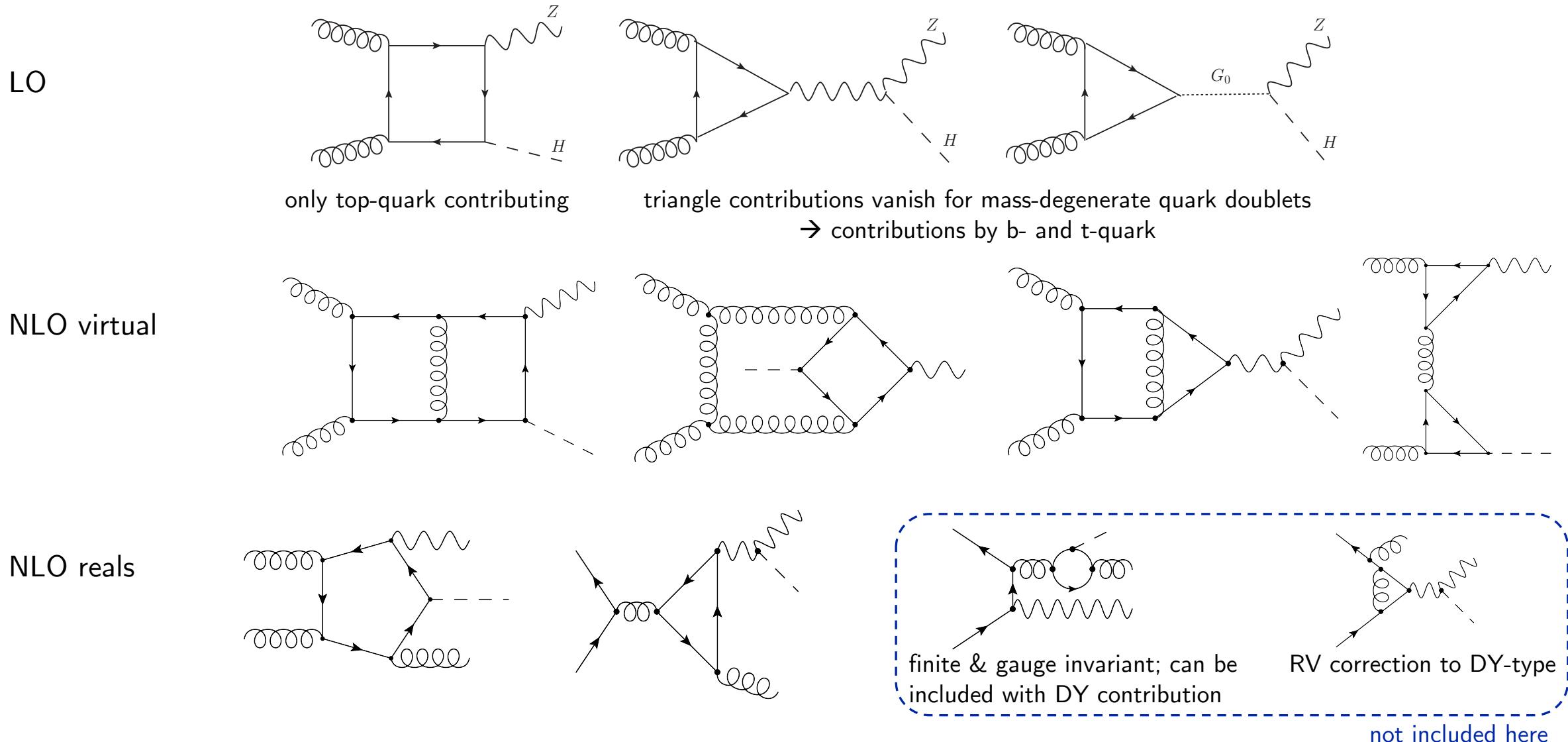
Full NLO results:

- Chen, Davies, Heinrich, Jones, MK, Mishima, Schlenk, Steinhauser 22



- Degrassi, Gröber, Vitti, Zhao 22
- small  $m_Z, m_H$  expansion  
Wang, Xu, Xu, Yang 21

# Introduction – ZH in Gluon Fusion



# Overview of Calculation

Virtual Corrections using 2 methods:

Numerical evaluation using pySecDec  
[Chen, Heinrich, Jones, MK, Klappert, Schlenk 20]

- ✓ valid for arbitrary kinematics
- evaluation challenging in HE region
- masses fixed during integral reduction
- can only use OS mass

High-energy expansion  
[Davies, Mishima, Steinhauser 20]

- only valid in HE region
- ✓ fast evaluation
- ✓ arbitrary masses

→ We combine these calculations at histogram level, using  $p_T = 200$  GeV as a threshold

Real-radiation amplitudes generated with Gosam [Cullen et.al.]

# Polarized Amplitudes

$$\mathcal{A} = \varepsilon_{\lambda_1}^{\mu_1}(p_1) \varepsilon_{\lambda_2}^{\mu_2}(p_2) (\varepsilon_{\lambda_3}^{\mu_3}(p_3))^* \mathcal{A}_{\mu_1\mu_2\mu_3}$$

$$g(p_1) + g(p_2) \rightarrow Z(p_3) + H(p_4)$$

Polarization vectors can be constructed from external momenta [L. Chen 19]

choose

$$\varepsilon_x^\mu = \mathcal{N}_x (-s_{23}p_1^\mu - s_{13}p_2^\mu + s_{12}p_3^\mu),$$

$$\varepsilon_y^\mu = \mathcal{N}_y (\epsilon_{\mu_1\mu_2\mu_3}^\mu p_1^{\mu_1} p_2^{\mu_2} p_3^{\mu_3}),$$

$$\begin{aligned} \varepsilon_T^\mu = \mathcal{N}_T & \left( (-s_{23}(s_{13} + s_{23}) + 2m_Z^2 s_{12}) p_1^\mu + (s_{13}(s_{13} + s_{23}) - 2m_Z^2 s_{12}) p_2^\mu \right. \\ & \left. + s_{12}(-s_{13} + s_{23}) p_3^\mu \right), \end{aligned}$$

$$\varepsilon_l^\mu = \mathcal{N}_l (-2m_Z^2 (p_1^\mu + p_2^\mu) + (s_{13} + s_{23}) p_3^\mu),$$

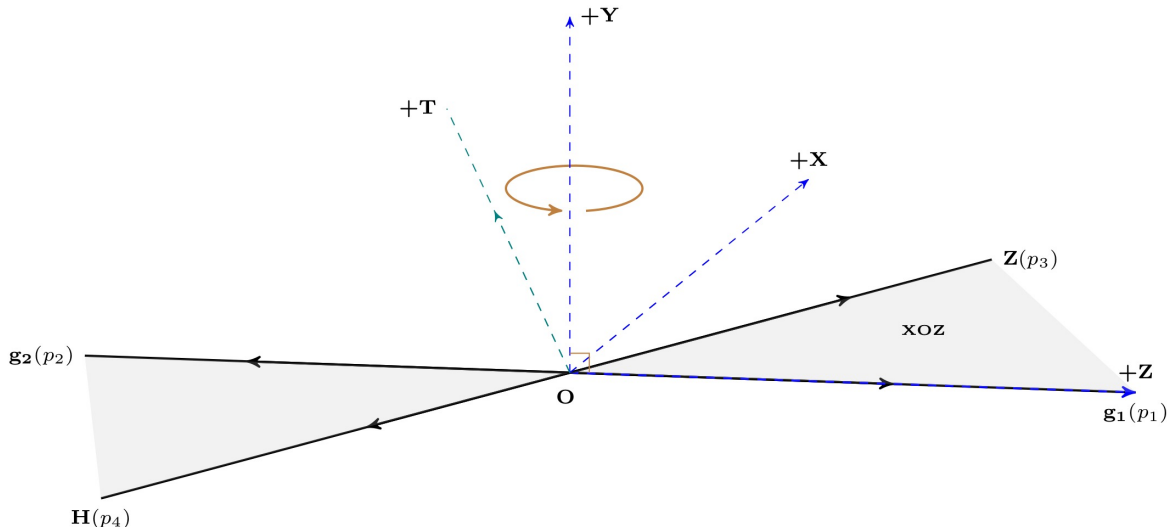
such that

$$\{\varepsilon_x, \varepsilon_y\} \cdot \{p_1, p_2\} = 0, \quad \{\varepsilon_y, \varepsilon_T, \varepsilon_l\} \cdot p_3 = 0, \quad \varepsilon_i^2 = -1$$

Can be used as polarization vectors of gluons and Z, respectively

circular polarizations:

$$\varepsilon_\pm^{\mu_1}(p_1) = \frac{1}{\sqrt{2}} (\varepsilon_x^{\mu_1} \pm i\varepsilon_y^{\mu_1}) \quad \varepsilon_\pm^{\mu_2}(p_2) = \frac{1}{\sqrt{2}} (\varepsilon_x^{\mu_2} \mp i\varepsilon_y^{\mu_2}) \quad \varepsilon_\pm^{\mu_3}(p_3) = \frac{1}{\sqrt{2}} (\varepsilon_T^{\mu_3} \pm i\varepsilon_y^{\mu_3})$$



6 polarization configurations:

$$\begin{array}{ll} \mathcal{P}_1^{\mu_1\mu_2\mu_3} = \varepsilon_x^{\mu_1} \varepsilon_x^{\mu_2} \varepsilon_y^{\mu_3}, & \mathcal{P}_2^{\mu_1\mu_2\mu_3} = \varepsilon_x^{\mu_1} \varepsilon_y^{\mu_2} \varepsilon_T^{\mu_3} \\ \mathcal{P}_3^{\mu_1\mu_2\mu_3} = \varepsilon_x^{\mu_1} \varepsilon_y^{\mu_2} \varepsilon_l^{\mu_3}, & \mathcal{P}_4^{\mu_1\mu_2\mu_3} = \varepsilon_y^{\mu_1} \varepsilon_x^{\mu_2} \varepsilon_T^{\mu_3} \\ \mathcal{P}_5^{\mu_1\mu_2\mu_3} = \varepsilon_y^{\mu_1} \varepsilon_x^{\mu_2} \varepsilon_l^{\mu_3}, & \mathcal{P}_6^{\mu_1\mu_2\mu_3} = \varepsilon_y^{\mu_1} \varepsilon_y^{\mu_2} \varepsilon_y^{\mu_3} \end{array}$$

# Integral Reduction

Use Integration-by-Parts Identities [[Chetyrkin, Tkachov; Laporta](#)]  
to express appearing 2-loop integrals in terms of master integrals.

~13.000 unreduced integrals → 452 masters

Reduction is quite challenging, can be simplified by fixing mass ratios

→ Eliminates 2 of the 5 mass scales  $s, t, m_t, m_Z, m_H$

Obtained using the programs:

- Kira [[Klappert, Lange, Maierhöfer, Usovitsch](#)]
- Firefly [[Klappert, Klein, Lange](#)]

→ uses finite-field methods to avoid large intermediate expressions

$$\int d^d p_i \frac{\partial}{\partial p_i^\mu} [q^\mu \mathbf{I}'(p_1, \dots, p_l; k_1, \dots, k_m)] = 0$$

$$\frac{m_Z^2}{m_t^2} = \frac{23}{83}, \quad \frac{m_H^2}{m_t^2} = \frac{12}{23}$$

# Choice of Master Integrals

- Use a (quasi-)finite basis of master integrals [von Manteuffel, Panzer, Schabinger 14]
  - simplifies numerical evaluation of integrals
  - poles in  $\varepsilon$  only in coefficients
  - requires integrals in shifted dimensions [Bern, Dixon, Kosower 92; Tarasov 96; Lee 10]
- Further improvements of integral basis to achieve:  
(by trying different basis choices for each sector)
  - $d$ -dependence factorizes from kinematic dependence in denominators of reduction coefficients  
[Smirnov, Smirnov `20; Usovitsch `20]
  - simple denominator factors  $D_1, D_2$
  - avoid poles in coefficients of integrals in top-level sectors as far as possible
  - small file-size of reductions

$$\frac{N(s, t, d)}{D_1(d)D_2(s, t)}$$

→ Some spurious poles & cancellations between integrals can be avoided

→ Reduced File sizes of expressions

- Amplitude: factor of 5 improvement
- Largest coefficient (double-tadpole): 150 MB → 5 MB

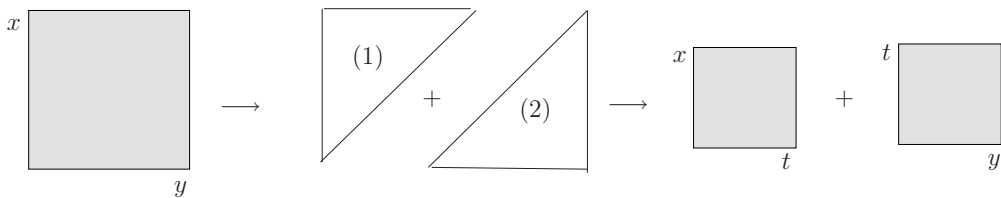
# Loop Integrals – Sector Decomposition

Numerical evaluation of loop integrals with pySecDec

[Borowka, Heinrich, Jahn, Jones, MK, Langer, Magerya, Pöldaru, Schlenk, Villa]

Available at  
[github.com/gudrunhe/secdec](https://github.com/gudrunhe/secdec)

- Sector decomposition [Binoth, Heinrich 00]  
factorizes overlapping singularities



- Subtraction of poles & expansion in  $\epsilon$
- Contour deformation [Soper 00; Binoth et.al. 05, Nagy, Soper 06; Borowka et al. 12]
  - Finite integrals at each order in  $\epsilon$
  - Numerical integration possible

New release:

- expansion by regions
- evaluation of linear combinations of integrals, with automated optimization of sampling points per sector
- automated reduction of contour-def. parameter
- automatically adjusts FORM settings

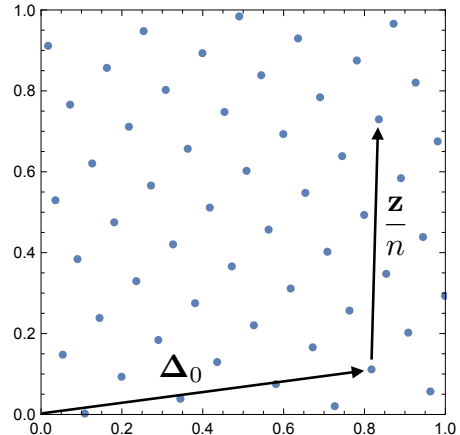
pySecDec integral libraries can be directly linked to amplitude code

# pySecDec – Quasi-Monte Carlo

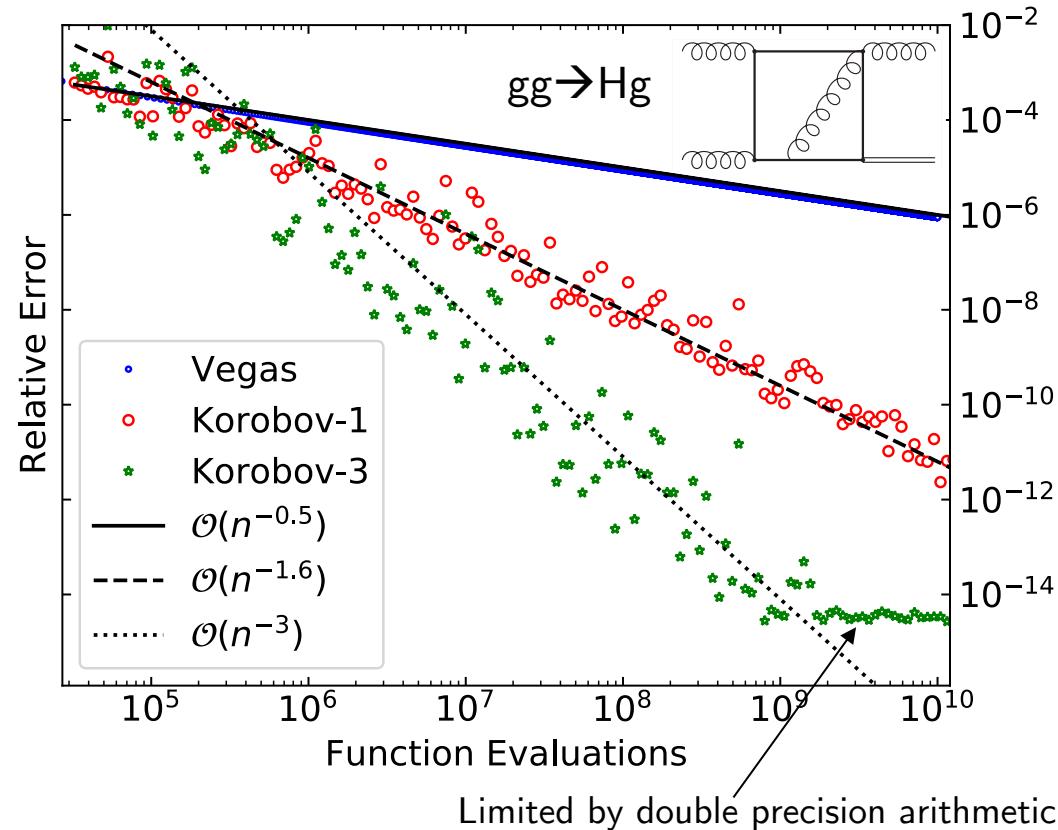
Our preferred integration algorithm is a  
Quasi-Monte Carlo using rank-1 shifted lattice rule

$$I[f] \approx I_k = \frac{1}{N} \cdot \sum_{i=1}^N f(\mathbf{x}_{i,k}), \quad \mathbf{x}_{i,k} = \left\{ \frac{i \cdot \mathbf{z}}{N} + \Delta_k \right\}$$

- $\{\dots\}$  = fractional part ( $\rightarrow x \in [0; 1]$ )
- $\Delta_k$  = randomized shifts
  - $\rightarrow m$  different estimates of Integral
  - $\rightarrow$  error estimate of result
- $\mathbf{z}$  = generating vector  
constructed component-by-component [Nuyens 07]  
minimizing worst-case error
- $\rightarrow$  integration error scales as  $\mathcal{O}(n^{-1})$  or better



Integrator available at [github.com/mppmu/qmc](https://github.com/mppmu/qmc)  
[Borowka, Heinrich, Jahn, Jones, MK, Schlenk]



# Evaluation of Amplitude

After sector decomposition and expansion in  $\varepsilon \rightarrow$  amplitude written in terms of 19.530 finite integrals

Optimizations to reduce run time:

- dynamically set n for each integral, minimizing

$$T = \sum_{\text{integral } i} t_i + \lambda \left( \sigma^2 - \sum_i \sigma_i^2 \right) \quad \sigma_i = c_i \cdot t_i^{-e}$$

$\sigma_i$  = error estimate (including coefficients in amplitude)  
 $\lambda$  = Lagrange multiplier       $\sigma$  = precision goal

- avoid reevaluation of integrals for different orders in  $\varepsilon$  and form factors

$$F^a = \sum_i \left[ \left( \sum_j C_{i,j}^a \varepsilon^j \right) \cdot \left( \sum_k I_{i,k} \varepsilon^k \right) \right] = \frac{C_{1,-2}^a \overset{\text{compute once}}{\cancel{I_{1,0}}} + C_{1,-1}^a I_{1,-1} + \dots}{\varepsilon^2} + \frac{C_{1,-1}^a \overset{\text{compute once}}{\cancel{I_{1,0}}} + \dots}{\varepsilon^1} + \dots$$

- parallelization on GPUs

typical run-time to obtain virtual amplitude with 0.3% precision:

2h using 2x Nvidia Tesla V100 GPUs

# High-Energy Expansion

Davies, Mishima, Steinhauser 20

Scale hierarchy in high-energy region:

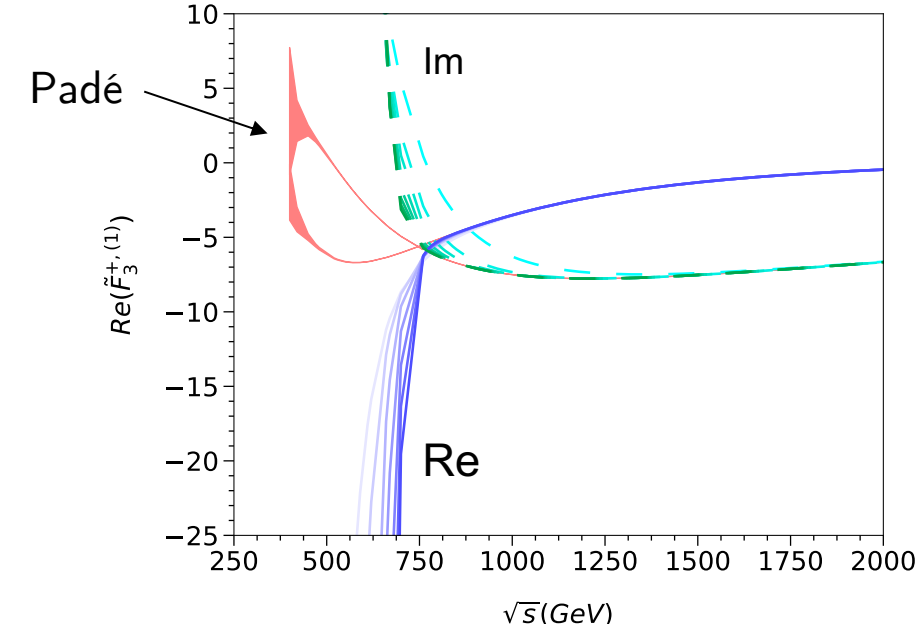
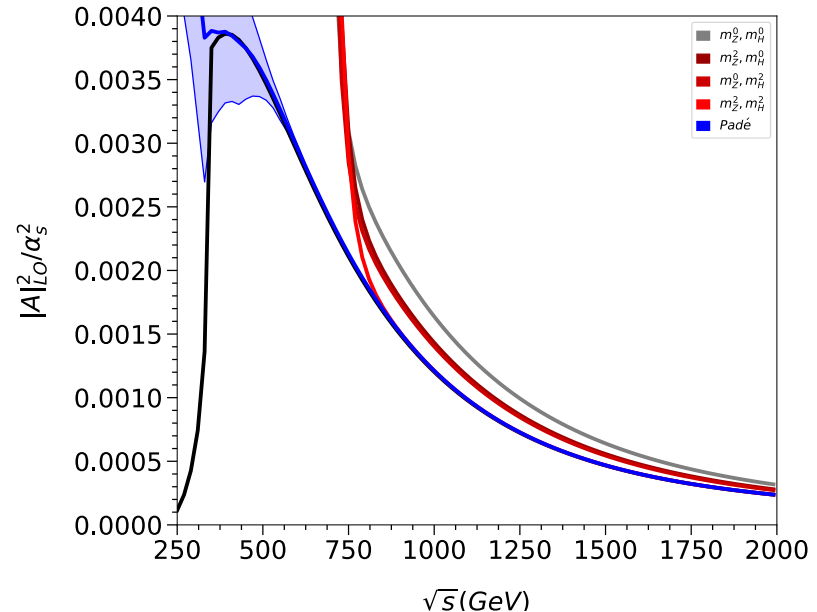
$$m_Z, m_H < m_t \ll s, t$$

- 1) Use Taylor series expansion in  $m_Z, m_H$   
→ remaining integrals only depend on  $m_t, s, t$
- 2) Solve differential equations using ansatz

$$I = \sum_{n_1=n_1^{\min}}^{\infty} \sum_{n_2=n_2^{\min}}^{\infty} \sum_{n_3=0}^{2l+n_1} c(I, n_1, n_2, n_3, s, t) \epsilon^{n_1} (m_t^2)^{n_2} (\log(m_t^2))^{n_3}$$

- 3) Boundary conditions using [see Mishima 18]
  - expansion-by-regions [Beneke, Smirnov; Jantzen]
  - Mellin-Barnes techniques
- 4) Series convergence improved using Padé approximants:

$$\mathcal{V}_{\text{fin}}^N = \frac{a_0 + a_1 x + \dots + a_n x^n}{1 + b_1 x + \dots + b_m x^m} \equiv [n/m](x)$$

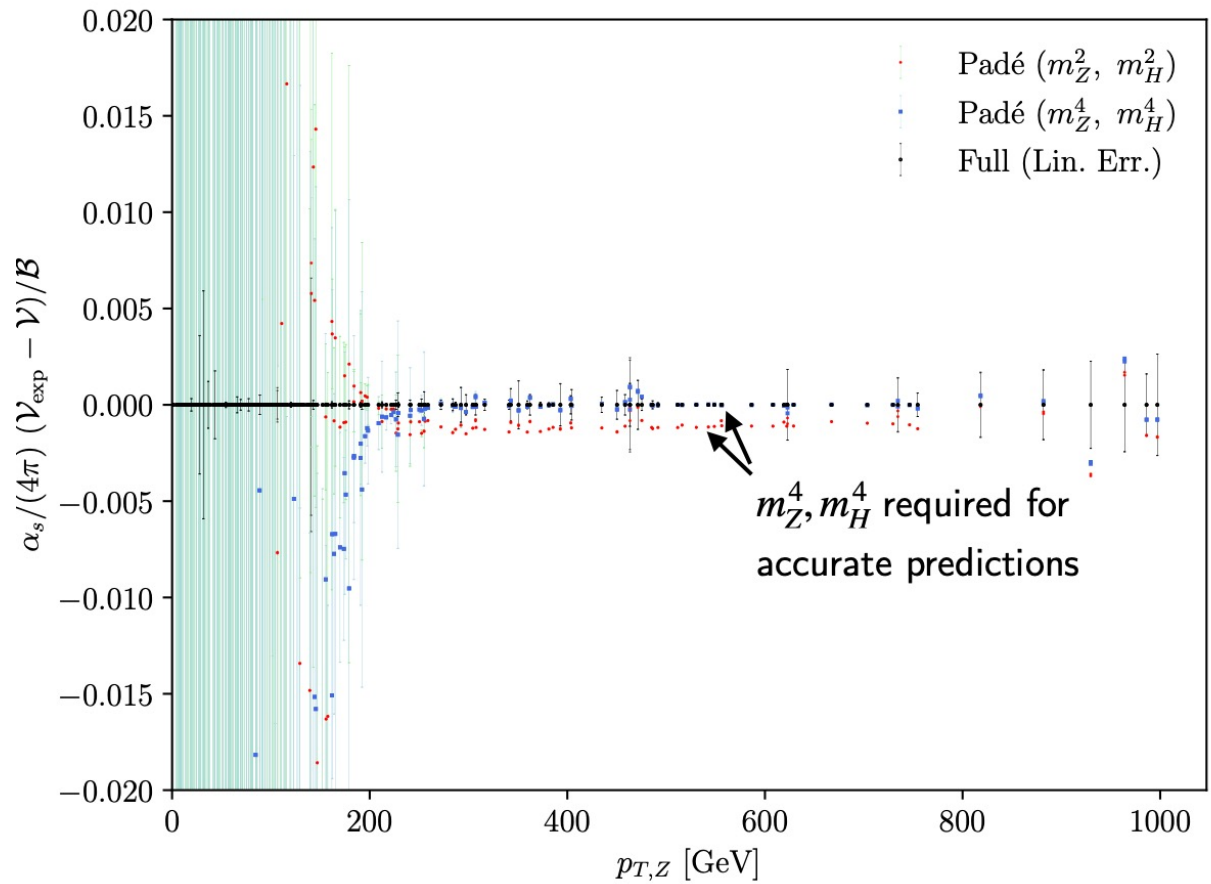


# Combination with Expansions

Comparison of numerical results with high-energy expansion

- expansion around small masses up to  $m_t^{32}, m_Z^4, m_H^4$
- agreement at 0.1% level or better for  $p_T > 200$  GeV
- $m_Z^4, m_H^4$  terms required to reach this accuracy

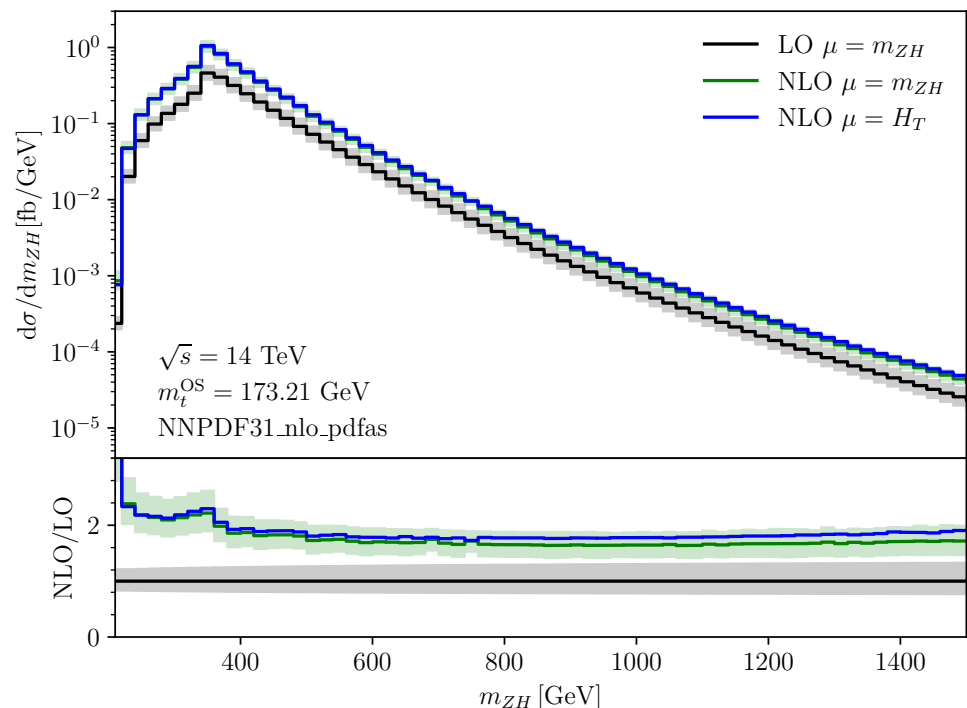
We switch from the numerical calculation  
to the expansion at  $p_T = 200$



# Results – Total Cross Section & Invariant Mass

$\sqrt{s}$	LO [fb]	NLO [fb]
13 TeV	$52.42^{+25.5\%}_{-19.3\%}$	$103.8(3)^{+16.4\%}_{-13.9\%}$
13.6 TeV	$58.06^{+25.1\%}_{-19.0\%}$	$114.7(3)^{+16.2\%}_{-13.7\%}$
14 TeV	$61.96^{+24.9\%}_{-18.9\%}$	$122.2(3)^{+16.1\%}_{-13.6\%}$

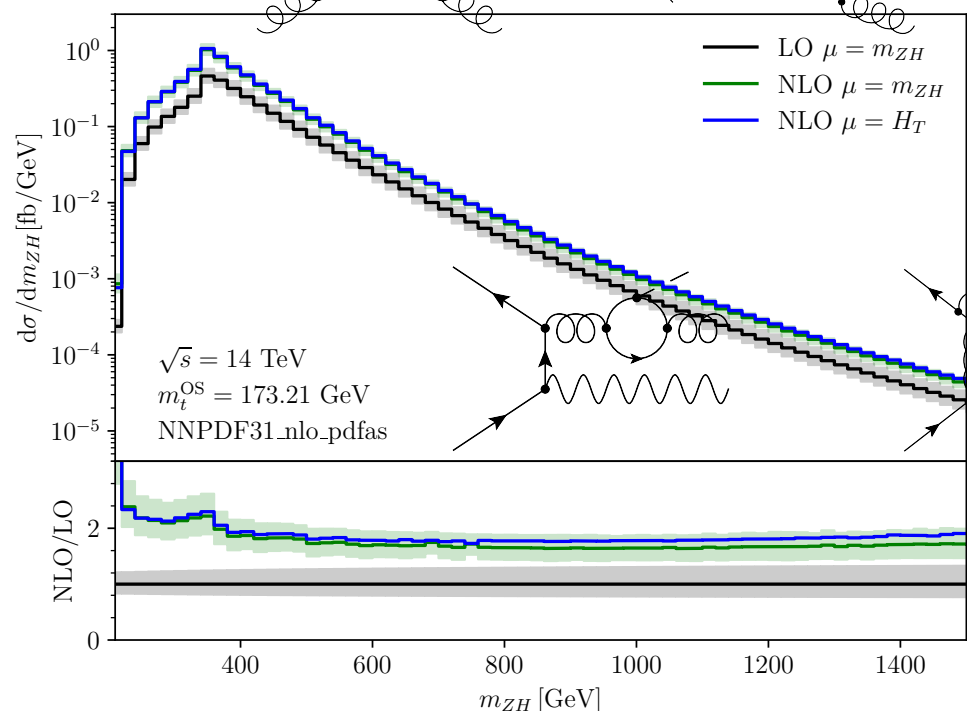
- NLO/LO  $\approx 2$
- NLO scale uncertainty:  $\pm 15\%$
- K-factor relatively flat for  $m_{ZH} > 400\text{GeV}$   
larger effects at top-pair threshold and below



# Results – Total Cross Section & Invariant Mass

$\sqrt{s}$	LO [fb]	NLO [fb]
13 TeV	$52.42^{+25.5\%}_{-19.3\%}$	$103.8(3)^{+16.4\%}_{-13.9\%}$
13.6 TeV	$58.06^{+25.1\%}_{-19.0\%}$	$114.7(3)^{+16.2\%}_{-13.7\%}$
14 TeV	$61.96^{+24.9\%}_{-18.9\%}$	$122.2(3)^{+16.1\%}_{-13.6\%}$

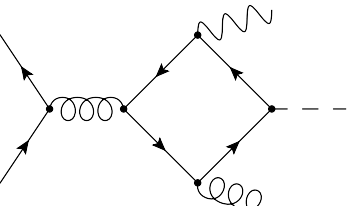
- NLO/LO  $\approx 2$
- NLO scale uncertainty:  $\pm 15\%$
- K-factor relatively flat for  $m_{ZH} > 400\text{GeV}$   
larger effects at top-pair threshold and below



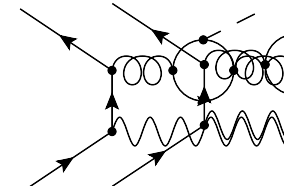
21.9.22

ZH production in gluon fusion, Matthias Kerner

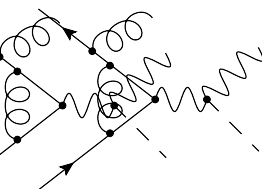
There is some freedom, which diagrams to include in  $q\bar{q}$  real radiation



part of  $gg \rightarrow ZH$



can best attributed to  
 $gg \rightarrow ZH$  or DY

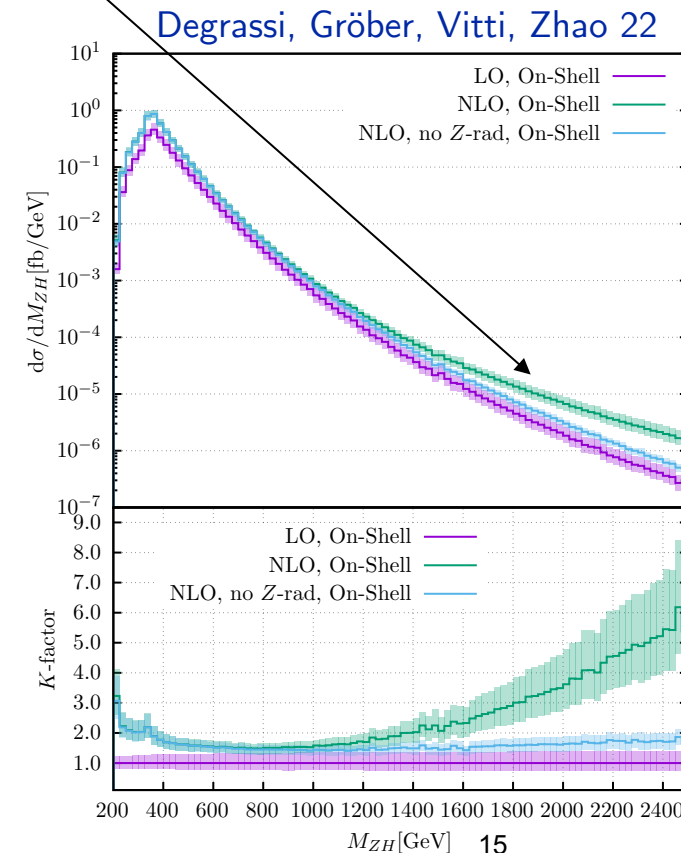


part of DY ZH production

We only include diagrams, where Z is radiated from closed quark loop

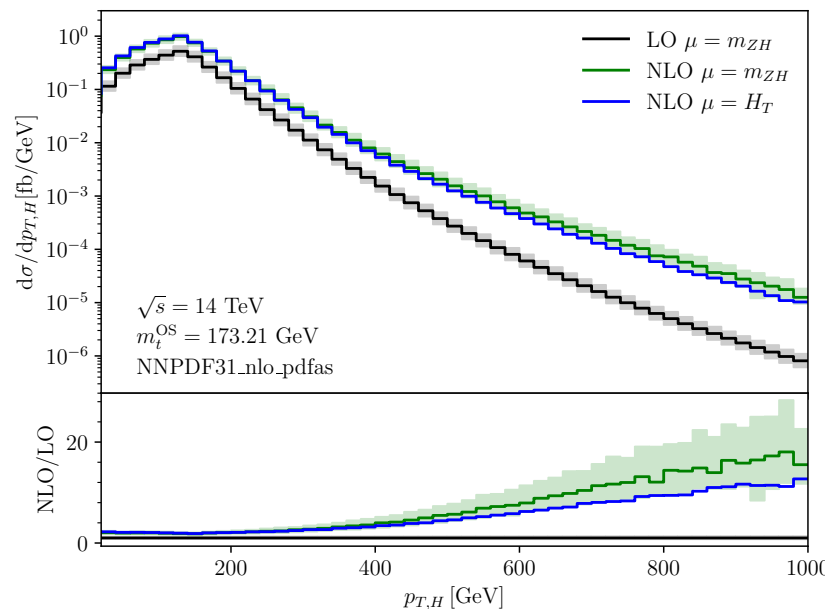
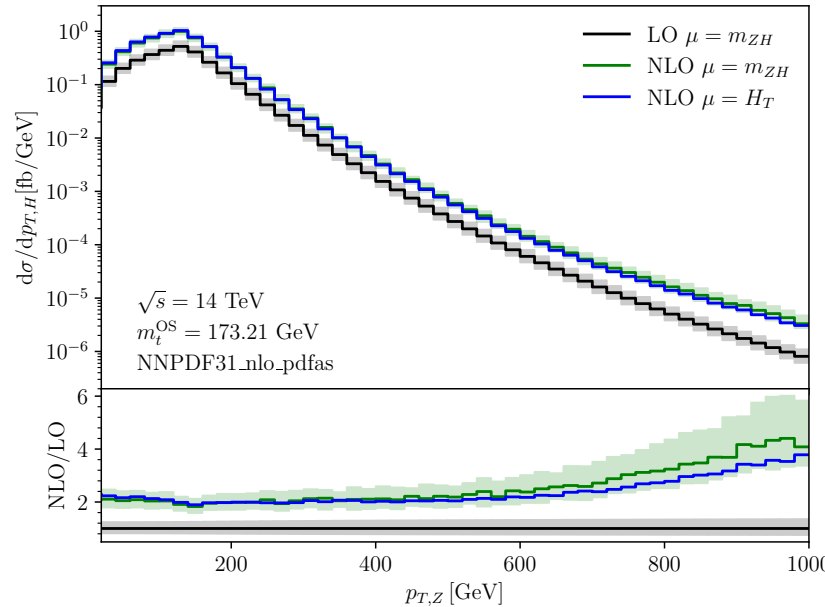
2<sup>nd</sup> class has been studied as  
part of NNLO  $q\bar{q} \rightarrow ZH$  production  
see e.g. Brein, Harlander, Wiesemann, Zirke 12

included in independent  
calculation of  $gg \rightarrow ZH$  production  
(formally N3LO of DY type)  
Degrassi, Gröber, Vitti, Zhao 22



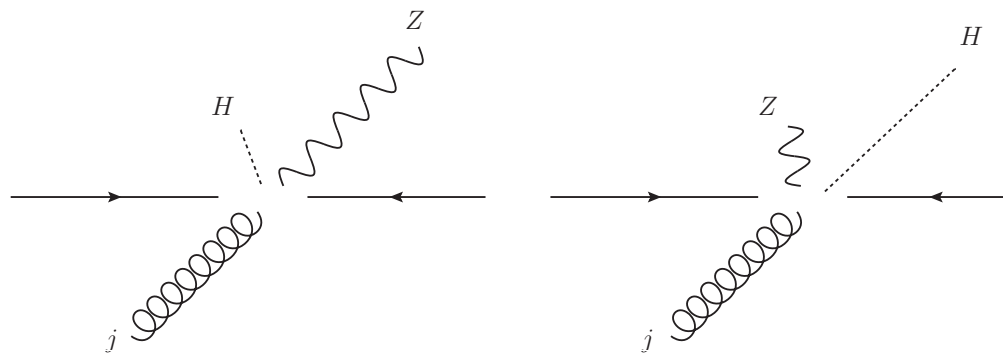
15

# Results – $p_T$ distributions



large corrections at high  $p_T$

caused by new kinematic region in real radiation:



difference of eikonal factors:

soft Z emission:  $\frac{p^\mu}{p \cdot p_Z}$

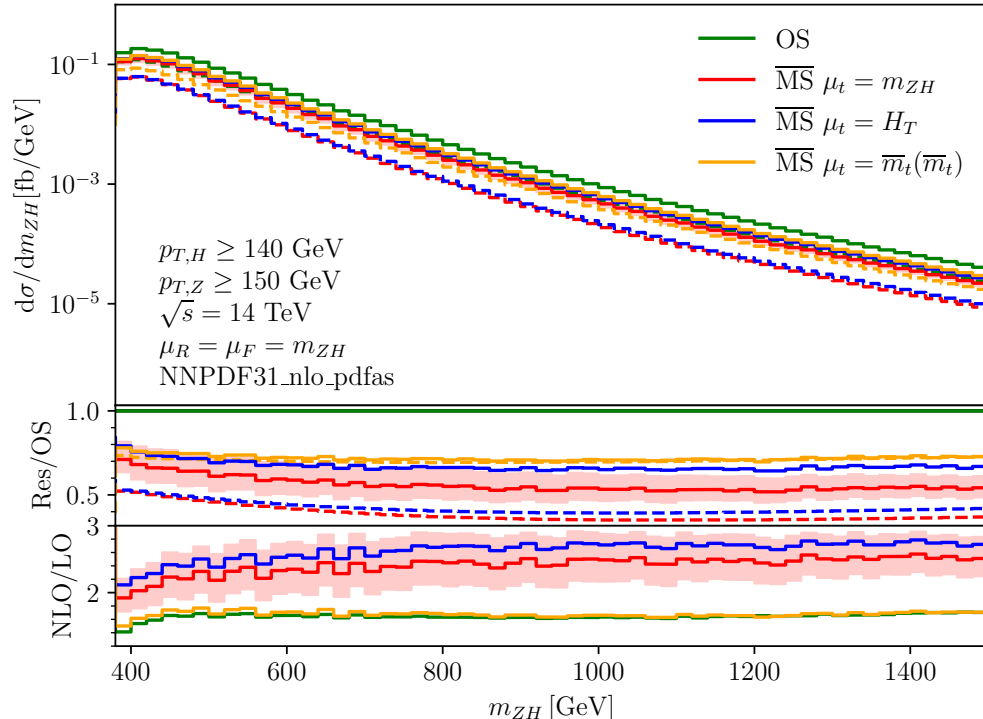
soft H emission:  $\frac{m_t}{p \cdot p_H}$

already observed in ZHj@LO  
 Hespel, Maltoni, Vryonidou 15; Les Houches 19

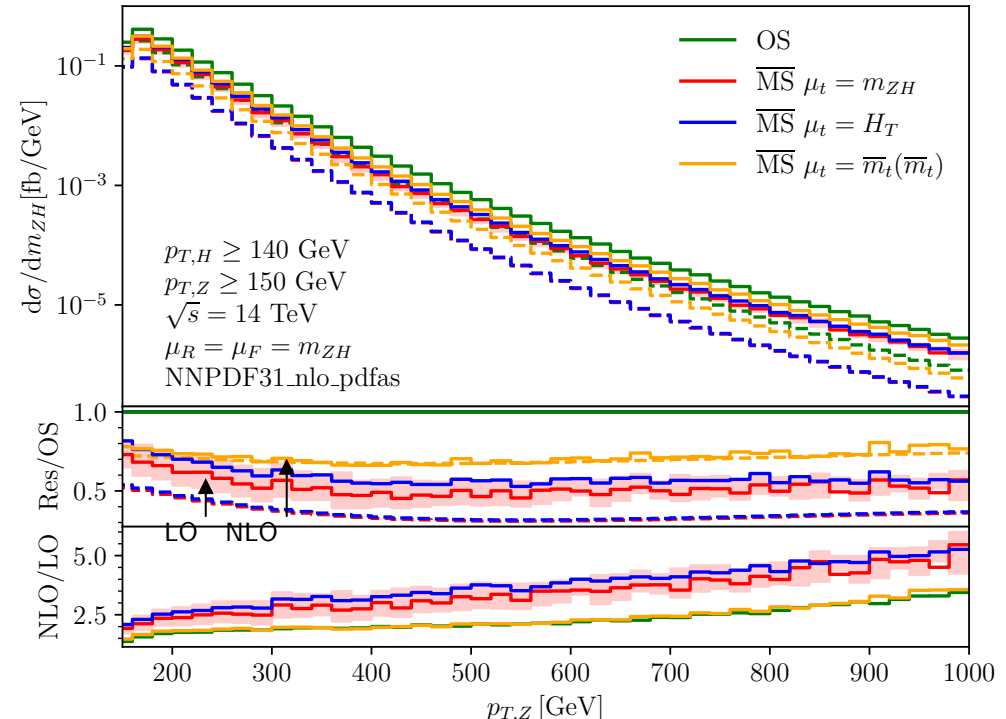
→ larger enhancement of  
 Z emission for large  $p_T$

# Mass Scheme Dependence

The results presented so far use OS renormalization of  $m_t$ ,  
 we can change to  $\overline{\text{MS}}$  renormalization  
 (using the high-energy expansion where  $m_t$  is not fixed in reduction)



$$m_t \rightarrow \overline{m}_t(\mu_t) \left( 1 + \frac{\alpha_s(\mu_R)}{4\pi} C_F \left\{ 4 + 3 \log \left[ \frac{\mu_t^2}{\overline{m}_t(\mu_t)^2} \right] \right\} \right)$$



The  $\overline{\text{MS}}$  result is significantly smaller than OS result:

LO: ~ factor 2.9    at  $m_{ZH} = 1 \text{ TeV}$   
 NLO: ~ factor 1.9

If taken as uncertainty, it is much larger than scale dependence

# Mass Scheme Dependence

Leading HE contributions in  $gg \rightarrow HH$  and  $gg \rightarrow ZH$  production

$$A_i^{\text{fin}} = a_s A_i^{(0),\text{fin}} + a_s^2 A_i^{(1),\text{fin}} + \mathcal{O}(a_s^3)$$

HH

$$A_i^{(0)} \sim m_t^2 f_i(s, t)$$

$$A_i^{(1)} \sim 6C_F A_i^{(0)} \log \left[ \frac{m_t^2}{s} \right]$$

LO:  $m_t^2$  from  $y_t^2$

NLO: leading  $\log(m_t^2)$  from mass c.t.  
converting to  $\overline{MS}$  gives  $\log(\mu_t^2/s)$   
motivating scale choice of  $\mu_t^2 = s$

ZH

$$A_i^{(0)} \sim m_t^2 f_i(s, t) \log^2 \left[ \frac{m_t^2}{s} \right],$$

$$A_i^{(1)} \sim \frac{(C_A - C_F)}{6} A_i^{(0)} \log^2 \left[ \frac{m_t^2}{s} \right]$$

LO: one  $m_t$  from  $y_t$

NLO: leading  $\log(m_t^2)$  not coming  
from mass c.t.

→ The leading contributions seem to have different origins for the 2 processes

It would be interesting to understand these logarithms in more detail.

(for some recent progress for off-shell H production, see [Liu, Modi, Penin 21; Mazzitelli 22](#))

# Conclusion

NLO corrections to ZH production in gluon-fusion

Virtual corrections obtained from combination of 2 calculations

- numeric evaluation using pySecDec
- high-energy expansion

Phenomenological results

- K-factor  $\approx 2$
- large corrections at high- $p_T$  due to new kin. configurations
- large dependence on top-mass renormalization scheme

Thank you for your attention!